Interfacial Tension between Coexisting Isotropic and Nematic Phases for a Lyotropic Polymer Liquid Crystal: Poly(*n*-hexyl isocyanate) Solutions

Wei-liang Chen and Takahiro Sato*

Department of Macromolecular Science, Osaka University, 1-1 Machikaneyama-cho, Toyonaka, Osaka 560-0043, Japan

Akio Teramoto

Research Organization of Science and Engineering, Ritsumeikan University, Nojihigashi 1-1-1, Kusatsu, Siga 525-8577, Japan

Received May 1, 1998; Revised Manuscript Received July 17, 1998

ABSTRACT: The interfacial tension γ between the coexisting isotropic and nematic phases of toluene solutions of poly(*n*-hexyl isocyanate) (PHIC) was determined as a function of the molecular weight of PHIC by the pendant drop method. The value of γ was almost independent of the molecular weight, in contrast to the theoretical prediction for rodlike polymer solutions that γ should be inversely proportional to the polymer molecular weight. This is consistent with the disagreement between rod theories and experiment with respect to the isotropic−nematic binodal concentrations of PHIC solutions and implies the importance of the chain-flexibility effect on γ in the solutions.

Interfacial properties play important roles in the kinetics of the phase separation and the morphology of phase-separating systems. In recent years, they have been extensively studied for many phase-separating polymer systems (e.g., polymer blends, polymer solutions, and block copolymers) by various experimental techniques.[1] Among the interfaces in those systems, the isotropic−liquid-crystal interface in lyotropic liquid-crystalline polymers is unique because it is accompanied by steep gradients of composition and degree of orientation. The interfacial tension in those systems determines the direction of the molecular alignment in the liquid-crystal phase in the vicinity of the interface.

Recently, we[2] measured the interfacial tension γ between the coexisting isotropic and nematic phases in a toluene solution of a poly(*n*-hexyl isocyanate) (PHIC) sample; PHIC is a typical semiflexible polymer, and its solution properties have been extensively studied so far.[3−5] The value of γ was about twice as large as γ calculated by the theory of Doi and Kuzuu[6] for solutions of hard rods. This disagreement may be ascribed to the effect of the flexibility of PHIC chains, which is known to strongly affect the isotropic−nematic phase equilibrium behavior in this system.[3,7]

To examine the chain flexibility effect on γ, the present study investigated the molecular weight dependence of γ for toluene solutions of PHIC. The results are compared with theories for stiff-polymer solutions in the rod and coil limits.

Experimental Section

PHIC Samples. Five fractionated PHIC samples (R-4, S-3, K-2, L-2, and M-2) were used for phase separation experiments and interfacial tension measurements. Samples K-2 and L-2 were obtained by fractionating a PHIC sample degraded with trifluoroacetic acid,[8] samples R-4 and M-2 were selected from our stock, and sample S-3 was the one used in the previous work.[2] The weight-average molecular weight M_w of each sample was determined by light scattering using hexane or dichloromethane as the solvent, and the polydispersity index M_w/M_n by GPC using tetrahydrofurane as the eluent; the detailed procedure of light scattering measurements is described elsewhere.[4,9] The results obtained are listed in Table 1, along with the numbers of Kuhn statistical segments N calculated from M_w. The values of N indicate that the conformations of the present PHIC samples range from nearly rodlike to weakly winding. The values of M_w/M_n show narrow molecular-weight distributions of all the samples.

Table 1. Characteristics of PHIC Samples Used

sample	$M_w/10^4$	M_w/M_n[c]	N[d]
R-4	9.70[a]	1.06	1.77
S-3	6.24[a]	1.06	1.14
K-2	3.44[b]	1.05	0.628
L-2	1.96[b]	1.05	0.358
M-2	1.24[b]		0.226

[a] Determined by light scattering for hexane solutions. [b] Determined by light scattering for dichloromethane solutions. [c] Determined by GPC. [d] Calculated from the equation $N = M_w/2qM_L$ with wormlike chain parameters, $M_L = 740$ nm^{-1} and $q = 37$ nm, for PHIC in 25 °C toluene.[11]

Phase Separation Experiments. A biphasic test solution was prepared by mixing a PHIC sample with distilled toluene in a test tube and stirring the mixture by a magnetic chip for 1−2 days in a 25 °C air bath. Each solution was centrifuged at 4000 rpm at 25 °C in a Sorval RC centrifuge to achieve a complete phase separation, and the coexisting isotropic and nematic phases were separately taken out using pipets. An aliquot of each separated solution was freeze-dried to determine the binodal polymer concentration, and then each dried sample was redissolved in toluene to determine the intrinsic viscosity at 25 °C. In the following, the binodal concentration and intrinsic viscosity determined for the isotropic (nematic) phase will be denoted as c_I (c_A) and $[\eta]_I$ ($[\eta]_A$), respectively. The remaining isotropic and nematic solutions were used for interfacial tension measurements.

Interfacial Tension Measurements. The interfacial tension between coexisting isotropic and nematic phases for toluene solutions of PHIC was determined at 25 °C by the pendant drop method. The detailed procedure was described in the previous paper.[2]

S0024-9297(98)00697-4 CCC: $15.00
Published on Web 09/01/1998

Table 2. Results of Phase Separation Experiments and Interfacial Tension Measurements for Toluene Solutions of PHIC

	original solution		isotropic phase			nematic phase			
sample	c/g cm^{-3}	$[\eta]$/cm^3 g^{-1}	c_I/g cm^{-3}	$[\eta]_I$/cm^3 g^{-1}	$M_{v,I}/10^4$	c_A/g cm^{-3}	$[\eta]_A$/cm^3 g^{-1}	$M_{v,A}/10^4$	$\gamma(\infty)/10^{-3}$ N m^{-1}
R-4	0.201	3.19	0.191			0.210			0.029
S-3	0.209	1.93	0.203			0.221			0.026
S-3	0.210								0.024[a]
K-2	0.241	0.86	0.233	85	3.30	0.253	91	3.60	0.031
L-2	0.290	0.39	0.287	37	1.90	0.306	41	2.08	0.030
M-2	0.359	0.19	0.351	17	1.10	0.366	19	1.20	0.027

[a] Obtained in the previous work.[2]

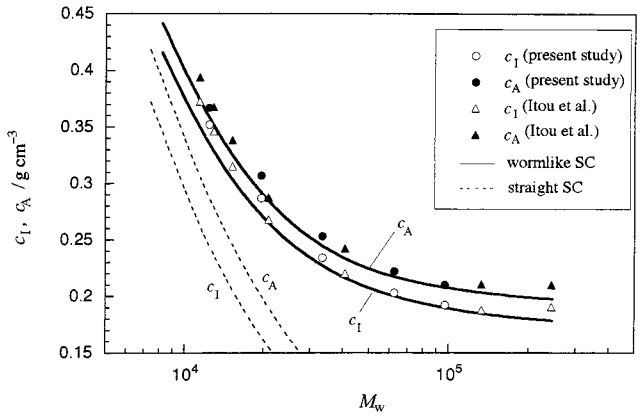

Figure 1. Molecular weight dependence of the binodal concentrations c_I and c_A for the PHIC−toluene system at 25 °C: (○, ●) data of the present work; (△, ▲) data of Itou et al.;[7] solid curves, calculated by the scaled particle theory for wormlike hard-spherocylinders (SC) with the persistence length $q = 37$ nm, the molar mass per unit contour length $M_L = 740$ nm^{-1}, and the hard-core diameter $d = 1.07$ nm; broken curves, calculated by the SPT for straight hard-spherocylinders (SC) with $M_L = 740$ nm^{-1} and $d = 1.07$ nm.[3]

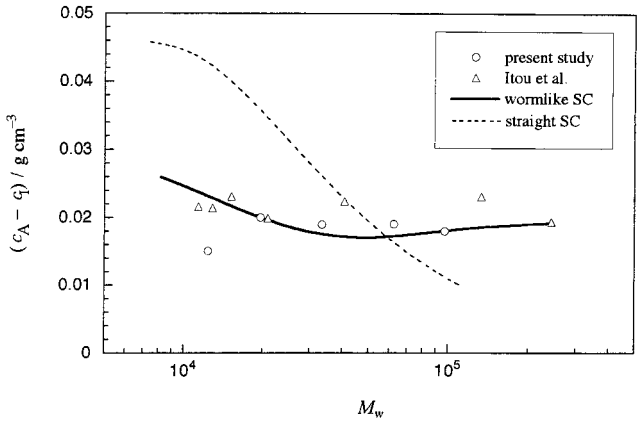

Figure 2. Molecular weight dependence of $c_A - c_I$ for the PHIC-toluene system: theoretical curves with the parameters the same as in Figure 1.

Results and Discussion

Coexisting Isotropic and Nematic Phases. Table 2 summarizes the results of the phase separation experiments for toluene solutions of five PHIC samples, obtained in the present study. Figure 1 compares our results for the binodal concentrations with the results of Itou and Teramoto[7] for the same system. Both data favorably compare with the theoretical results (solid curves) calculated by the scaled particle theory (SPT) for solutions of wormlike hard-spherocylinders.[3,10] Here the theory uses the molecular parameters previously determined for PHIC in toluene: the persistence length $q = 37$ nm, the molar mass per unit contour length $M_L = 740$ nm^{-1}, and the hard-core diameter $d = 1.07$ nm.[11−13] The broken curves in the figure show the theoretical values for c_I and c_A calculated by the SPT for solutions of *straight* hard-spherocylinders with $M_L = 740$ nm^{-1} and $d = 1.07$ nm. The disagreement of the hard-rod theory with the experimental results for PHIC solutions becomes remarkable with increasing the PHIC molecular weight, which demonstrates the strong effect of chain flexibility on the isotropic−nematic binodal concentrations through the conformational entropy loss of PHIC chains due to the nematic ordering.[3,14,15]

Since the interfacial tension is closely related to the concentration difference between the coexisting two phases (i.e., the phase gap) as mentioned below, we compare $c_A - c_I$ calculated from the experimental data listed in Table 2 with the theoretical results in Figure 2. Both the results of the experiment and the SPT for wormlike hard-spherocylinders are almost independent of M_w in the M_w range examined, and agreement between the two results is satisfactory, except for the lowest molecular weight sample M-2. The phase gap calculated from the theoretical results of the SPT for straight hard-spherocylinders is a decreasing function of the molecular weight and does not agree with the experimental results.

Table 2 also lists the intrinsic viscosities $[\eta]_I$ and $[\eta]_A$ in toluene for the PHIC samples recovered from the coexisting isotropic and nematic phases, respectively, and the viscosity-average molecular weights $M_{v,I}$ and $M_{v,A}$ estimated from $[\eta]_I$ and $[\eta]_A$, respectively, using the $[\eta]$−molecular weight relation of Itou et al.[11] For all the PHIC samples examined, $M_{v,A}$ is slightly larger than $M_{v,I}$; similar results were obtained for the same system by Itou and Teramoto.[7] This demonstrates that the molecular weight fractionation takes place at the phase separation, where the higher molecular weight components tend to distribute in the coexisting nematic phase in excess of the lower molecular weight components,[16] even though the samples used have considerably narrow molecular-weight distributions (cf. Table 1).

Interfacial Tension. Figure 3 shows an example of the meridian curve measured for a pendant drop of the nematic phase formed in the coexisting isotropic phase. Here, the x and y axes are chosen to coincide with the tangent and normal lines at the apex of the drop, respectively. The midpoints of horizontal segments cut by the meridian curve, indicated by the unfilled circles in Figure 3, are on the y axis, which guarantee the proper choice of the x and y axes.[2] By fitting the theoretical meridian curve calculated by the Young−Laplace equation to the experimental points,[2] we determined the radius of the curvature r_0 at the drop apex and the dimensionless shape factor β, both including in the Young−Laplace equation.

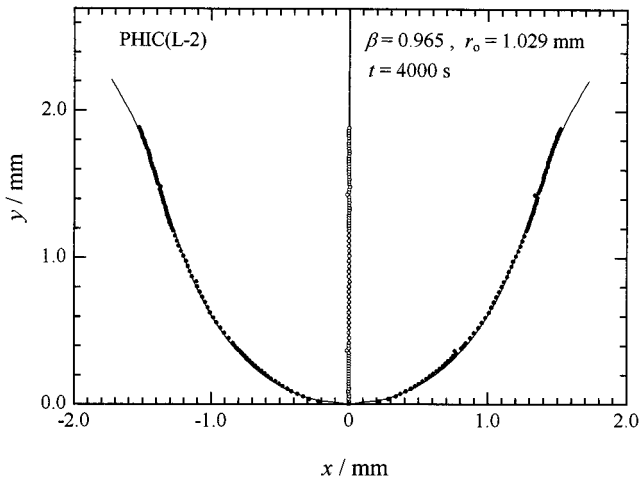

Figure 3. Meridian curve for a pendant drop of the nematic phase formed in the coexisting isotropic phase for a toluene solution of PHIC sample L-2 at 25 °C ($t = 4000$ s): filled circles, experimental data; curve, theoretical result obtained by least-squares regression; unfilled circles, midpoints of horizontal segments cut by the experimental meridian curve.

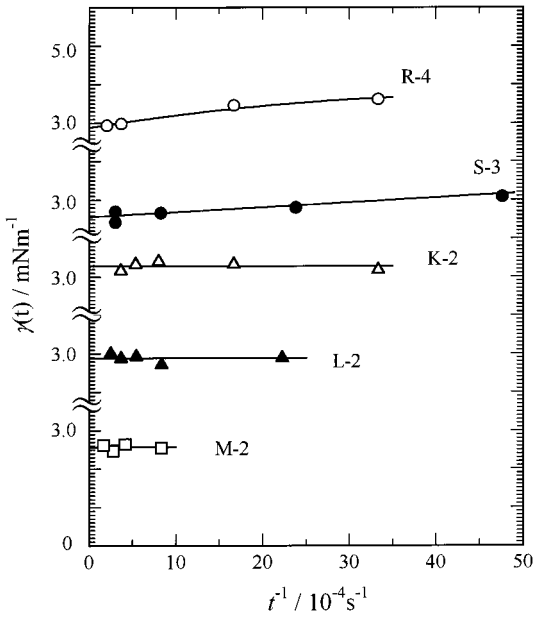

Figure 4. Plots of $\gamma(t)$ against t^{-1} for toluene solutions of five PHIC samples.

From the results of r_0 and β, the interfacial tension γ was calculated by the equation[17,18]

$$\gamma = (r_0^2/\beta)g\Delta\rho \qquad (1)$$

where g is the gravitational acceleration and $\Delta\rho$ is the density difference between the coexisting two phases. For each solution, $\Delta\rho$ was estimated from the binodal concentrations c_I and c_A determined by the phase separation experiments (cf. Table 2) using the density–concentration relation determined in the previous work.[2]

For higher molecular weight samples, the interfacial tension calculated by eq 1 decreased with the time t elapsed after forming the nematic drop from the microsyringe into the coexisting isotropic solution. To express explicitly this time dependence, the interfacial tension is denoted as $\gamma(t)$ in what follows. Figure 4 plots $\gamma(t)$ against t^{-1} for solutions of five PHIC samples examined. It can be seen that the time dependence of $\gamma(t)$ becomes more remarkable as the molecular weight of the PHIC samples increases. As demonstrated in the previous study,[2] PHIC chains in the nematic phase align parallel to the interface in the equilibrium state, owing to thermodynamical favorableness. The time dependence of $\gamma(t)$ shown in Figure 4 indicates that the approach to this equilibrium state is a rather slow process.

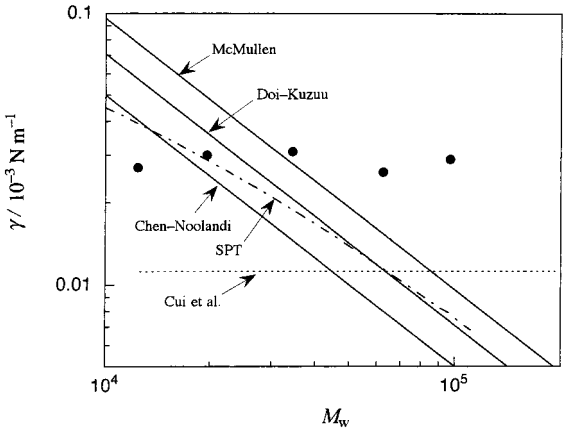

Figure 5. Comparison of γ for toluene solutions of PHIC with various theories:[6,21,24,28] solid and dash–dotted curves, calculated with $M_L = 740$ nm^{-1} and $d = 1.07$ nm; dotted line, calculated with $d = 1.07$ nm and $q = 37$ nm.

By extrapolating $\gamma(t)$ to infinite t (or $t^{-1} \rightarrow 0$ in Figure 4), we determined the equilibrium interfacial tension $\gamma(\infty)$ for each PHIC sample at 25 °C. The values of $\gamma(\infty)$ are listed in the tenth column of Table 2. The present result for sample S-3 is in good agreement with the previous result,[2] which indicates the reproducibility of $\gamma(\infty)$ measurements for this system by the pendant drop method. From the data in Table 2, it can be seen that $\gamma(\infty)$ is almost independent of the PHIC molecular weight, almost in parallel with the molecular weight dependence of the phase gap $c_A - c_I$ shown in Figure 2.

Comparison with Theories. The isotropic–nematic interfacial tension for hard rodlike polymer solutions was theoretically calculated by several workers.[6,19–24] Most of the theories utilized the free energy density expression of Onsager[25] for solutions of long hard-rods, which is based on the *second virial approximation*. The difference among those theories is the expressions for the interfacial profiles with respect to the concentration and degree of orientation, as well as of the orientational distribution function. Doi and Kuzuu[6] used trial functions of hyperbolic tangents for those profiles and the Onsager trial function for the orientational distribution function, while McMullen[21] expressed the orientational distribution function in a series of spherical harmonics with the expansion coefficients represented by hyperbolic tangent functions. More recently, Chen and Noolandi[24] calculated the equilibrium concentration and orientation profiles and also the orientational distribution function numerically, without assuming any specific functional forms.

Figure 5 compares the experimental results for $\gamma(\infty)$ for PHIC solutions (circles) with those theoretical results for hard rodlike polymers (solid curves). Here the theories used the same molecular parameters (M_L and d) as used above to calculate the binodal concentrations c_I and c_A. All the rod theories predict that the isotropic–nematic interfacial tension is inversely proportional to the polymer molecular weight, which is inconsistent with the experimental results.

The three theories shown in Figure 5 neglect the contributions to $\gamma(\infty)$ of the third and higher virial terms as well as of the noncrossed configuration[25,26] in the free energy density of the system. To assess the importance of those contributions to $\gamma(\infty)$, we have extended the Doi−Kuzuu theory by use of the scaled particle theory (SPT)[3,26] for straight hard-spherocylinders, without using the second virial approximation. This extension is described in the Appendix, and the results are shown by the dash−dotted curve in Figure 5. The difference between this theory and the original Doi−Kuzuu theory is appreciable in the low molecular weight region, and the theoretical results of the SPT are closer to the experimental data in this region. However, the agreement between the theory and experiment for $\gamma(\infty)$ is not improved in the high molecular weight region.

The interfacial tension is equal to the excess free energy of the biphasic system with a real continuous interface over that of the system with the hypothetical Gibbs dividing interface.[27] Since the difference between the two systems in the interfacial region disappears when the concentration and the degree of orientation become identical in the two coexisting phases, $\gamma(\infty)$ should be primarily correlated with the differences in the concentration and degree of orientation between the two phases. In fact, both the phase gap (in Figure 2) and $\gamma(\infty)$ (in Figure 5) consistently exhibit molecular weight independence. As shown in Figure 2, the agreement between experiment (circles) and the SPT for straight hard-spherocylinders (broken curve) with respect to the phase gap is much improved if the chain flexibility effect is taken into account in the theory (solid curve). From this result, it is plausible that the disagreement between the experiment and rod theories for γ also arises from the chain flexibility effect.

Cui et al.[28] and also Grosberg and Pachomov[29] calculated $\gamma(\infty)$ for solutions of wormlike chains *in the coil limit*. Figure 5 shows Cui et al.'s results with the persistence length $q = 37$ nm, by the dotted line. Although the molecular weight independence of $\gamma(\infty)$ is in accordance with the experimental results of the PHIC−toluene system, the absolute values of the theoretical $\gamma(\infty)$ are much smaller than the experimental values. At present, there are no theoretical calculations of γ for semiflexible polymer solutions with intermediate flexibility. We desire such a theoretical extension soon.

Acknowledgment. This work was supported by a Grant-in-Aid (0965099) for Scientific Resarch from the Ministry of Education, Science, Sport, and Culture of Japan. The authors are indebed to Prof. Z. Y. Chen at the University of Waterloo for pointing out ref 28.

Appendix

Doi and Kuzuu[6] calculated the isotropic−nematic interfacial tension γ for solutions of hard-rods on the basis of the Onsager theory,[25] which neglects the contributions of the third and higher virial terms as well as of the "noncrossed" configuration[25] to the free energy. In this appendix, we consider those contributions to the free energy by using the scaled particle theory (SPT) for straight hard-spherocylinders,[10,30,31] and assess their effects on γ.

Let us consider an inhomogeneous solution of hard-spherocylinders with the contour length L_c of the cylindrical part and the hard-core diameter d. When the generalized density distribution in the solution is represented by $\rho(\mathbf{x})$, where $\mathbf{x}$ denotes the set of the position vector $\mathbf{r}$ of the center of mass and the orientational unit vector $\mathbf{a}$ of a spherocylinder, the free energy functional $F[\rho(\mathbf{x})]$ may be expressed by[26]

$$\frac{F[\rho(\mathbf{x})]}{k_B T} = \int \rho(\mathbf{x})\{\ln[\rho(\mathbf{x})] - 1\}\, d\mathbf{x} - \frac{1}{2}\int d\mathbf{x}\, d\mathbf{x}'\, [H_A(\phi)\Phi_0(\mathbf{x},\mathbf{x}') + H_I(\phi)\Phi'_0(\mathbf{x},\mathbf{x}')]\rho(\mathbf{x})\rho(\mathbf{x}') \quad \text{(A.1)}$$

where Φ_0 and Φ'_0 are the Mayer functions with respect to the hard-core potential in the "crossed" and "noncrossed" configurations, respectively, and the factors $H_A(\phi)$ and $H_I(\phi)$ are defined by

$$H_A(\phi) \equiv \frac{1}{1-\phi}\left[1 + \frac{2(X'+1)\phi}{(3X'+2)(1-\phi)}\right] \quad \text{(A.2)}$$

$$H_I(\phi) = \frac{3}{4(1-\phi)^2}\left[1 - \frac{5X'^2 + 6X' + 2}{(3X'+1)^2}\phi\right] - \frac{\ln(1-\phi)}{4\phi} \quad \text{(A.3)}$$

with $X' \equiv L_c/d$ and the volume fraction ϕ of the spherocylinder. The factors $H_A(\phi)$ and $H_I(\phi)$ take into account the higher virial terms on the basis of the SPT.

According to Doi and Kuzuu,[6] we use the following trial function for $\rho(\mathbf{x})$ in the isotropic−nematic interfacial region:

$$\rho(\mathbf{x}) = c'(z) f(\alpha(z)\mathbf{a}\cdot\mathbf{n}) = c'(z)\frac{\alpha(z)\cosh(\alpha(z)\mathbf{a}\cdot\mathbf{n})}{4\pi \sinh \alpha(z)} \quad \text{(A.4)}$$

where

$$\begin{cases} c'(z) = c'_I + \frac{1}{2}(c'_A - c'_I)[\tanh(z/\xi) + 1] \\ \alpha(z) = \frac{1}{2}\alpha[\tanh(z/\xi) + 1] \end{cases} \quad \text{(A.5)}$$

In the above equations, $c'(z)$ and $\alpha(z)$ are the number concentration and degree of orientation, respectively, at the distance z from the Gibbs dividing surface, $f(\alpha(z)\mathbf{a}\cdot\mathbf{n})$ is the orientational distribution function of $\mathbf{a}$ around the director $\mathbf{n}$, c'_I, c'_A, and α are the equilibrium number concentrations of the coexisting isotropic and nematic phases and the equilibrium degree of orientation of the nematic phase, respectively. Equation A.5 contains a variational parameter ξ representing the thickness of the interfacial region, which should be determined so as to minimize the interfacial free energy. On the other hand, the bulk properties, c'_I, c'_A, and α, are determined from the minimization condition of the bulk free energy obtained from eq A1, as functions of L_c and d.[3]

Inserting this trial function into eq A.1, we have the free energy density $F(z)$ as

$$F(z)/k_B T = c'(z)\ln c'(z) + c'(z)\sigma_R(\alpha(z)) + 4H_I(\phi(z))\phi(z)c'(z) + \frac{\pi}{4}L_c^2 d H_A(\phi(z))c'(z)^2 \times \left[\rho(\alpha(z)) - \frac{1}{12}(L_c/\xi)^2\sum_{j=1}^{3}\tau_j(z)\right] \quad \text{(A.6)}$$

with

$$\begin{cases} \sigma_R(\alpha(z)) = \int f(\alpha(z)\mathbf{a}\cdot\mathbf{n}) \ln[4\pi f(\alpha(z)\mathbf{a}\cdot\mathbf{n})]\, d\mathbf{a} \\ \rho(\alpha(z)) = \frac{4}{\pi}\int d\mathbf{a} \int d\mathbf{a}'\, |\mathbf{a}\times\mathbf{a}'| f(\alpha(z)\mathbf{a}\cdot\mathbf{n}) f(\alpha(z)\mathbf{a}'\cdot\mathbf{n}) \\ \tau_1(z) \equiv \frac{4}{\pi}\int d\mathbf{a} \int d\mathbf{a}'\, a_z^2 |\mathbf{a}\times\mathbf{a}'| f_z(\alpha(z)\mathbf{a}\cdot\mathbf{n}) f_z(\alpha(z)\mathbf{a}'\cdot\mathbf{n}) \\ \tau_2(z) \equiv \frac{4}{\pi}[c'_z(z)/c'(z)] \int d\mathbf{a} \int d\mathbf{a}'\, (a_z^2 + a'^2_z) |\mathbf{a}\times\mathbf{a}'| f(\alpha(z)\mathbf{a}\cdot\mathbf{n}) f_z(\alpha(z)\mathbf{a}'\cdot\mathbf{n}) \\ \tau_3(z) \equiv \frac{4}{\pi}[c'_z(z)/c'(z)]^2 \int d\mathbf{a} \int d\mathbf{a}'\, a_z^2 |\mathbf{a}\times\mathbf{a}'| f(\alpha(z)\mathbf{a}\cdot\mathbf{n}) f(\alpha(z)\mathbf{a}'\cdot\mathbf{n}) \end{cases} \tag{A.7}$$

where $c'_z(z)$ and $f_z(\alpha(z)\mathbf{a}\cdot\mathbf{n})$ are the spatial differentiations of $c'(z)$ and $f(\alpha(z)\mathbf{a}\cdot\mathbf{n})$ toward the z direction (normal to the interface) and a_z is the z component of $\mathbf{a}$. The interfacial tension γ is calculated by

$$\gamma = \int_{-\infty}^{0} [F(z) - F_I]\, dz + \int_{0}^{\infty} [F(z) - F_A]\, dz \tag{A.8}$$

where F_I and F_A are the free energy densities of the isotropic and nematic bulk phases. The integrations appearing in eqs A.7 and A.8 are not possible analytically, and thus we made numerical calculations. The final result of γ can be written as

$$\gamma = \frac{k_B T}{d L_c} (K_c \cos^2 \mu + K_s \sin^2 \mu)^{1/2} \tag{A.9}$$

where $\mu = \cos^{-1}(\mathbf{a}\cdot\mathbf{n})$, and K_c and K_s are numerical constants depending on L_c and d. From numerical integrations, it turns out that K_c is larger than K_s, so that γ takes a minimum at $\mu = \pi/2$. Since the minimum value of γ is the equilibrium interfacial tension, we have

$$\gamma(\infty) = \frac{k_B T}{d L_c} K_s^{1/2} \tag{A.10}$$

If we input unity and zero for $H_A(\phi)$ and $H_I(\phi)$, respectively, we can reproduce the Doi−Kuzuu result: $K_c = 0.182$ and $K_s = 0.0660$.[6]

References and Notes

(1) *Physics of Polymer Surfaces and Interfaces*; Sanchez, I. C., Ed.; Butterworth-Neinemann: Boston, MA, 1992.
(2) Chen, W.-L.; Sato, T.; Teramoto, A. *Macromolecules* **1996**, *29*, 4283.
(3) Sato, T.; Teramoto, A. *Adv. Polym. Sci.* **1996**, *126*, 85.
(4) Jinbo, Y.; Sato, T.; Teramoto, A. *Macromolecules* **1994**, *27*, 6080.
(5) Ohshima, A.; Kudo, H.; Sato, T.; Teramoto, A. *Macromolecules* **1995**, *28*, 6095.
(6) Doi, M.; Kuzuu, N. *J. Appl. Polym. Sci., Appl. Polym. Symp.* **1984**, *41*, 65.
(7) Itou, T.; Teramoto, A. *Macromolecules* **1988**, *21*, 2225.
(8) Kuwata, M.; Murakami, H.; Norisuye, T.; Fujita, H. *Macromolecules* **1984**, *17*, 2731.
(9) Murakami, H.; Norisuye, T.; Fujita, H. *Macromolecules* **1980**, *13*, 345.
(10) Sato, T.; Teramoto, A. *Mol. Cryst. Liq. Cryst.* **1990**, *178*, 143.
(11) Itou, T.; Chikiri, H.; Teramoto, A.; Aharoni, S. M. *Polym. J.* **1988**, *20*, 143.
(12) Sato, T.; Teramoto, A. *Acta Polym.* **1994**, *45*, 399.
(13) Sato, T.; Jinbo, Y.; Teramoto, A. *Macromolecules* **1997**, *30*, 590.
(14) Khokhlov, A. R.; Semenov, A. N. *Physica* **1981**, *108A*, 546.
(15) Khokhlov, A. R.; Semenov, A. N. *Physica* **1982**, *112A*, 605.
(16) Flory, P. J.; Frost, R. S. *Macromolecules* **1978**, *11*, 1126.
(17) Andreas, J. M.; Hauser, E. A.; Tucker, W. B. *J. Phys. Chem.* **1938**, *42*, 1001.
(18) Rotenberg, Y.; Boruvka, L.; Neumann, A. W. *J. Colloid Interface Sci.* **1983**, *93*, 169.
(19) Murakami, J. *J. Phys. Soc., Jpn.* **1977**, *42*, 210.
(20) Kimura, H.; Nakano, H. *J. Phys. Soc., Jpn.* **1986**, *55*, 4186.
(21) McMullen, W. E. *Phys. Rev. A* **1988**, *38*, 6384.
(22) Holyst, R.; Poniewiesrski, A. *Phys. Rev. A* **1988**, *38*, 1527.
(23) Moore, B. G.; McMullen, W. E. *Phys. Rev. A* **1990**, *42*, 6042.
(24) Chen, Z. Y.; Noolandi, J. *Phys. Rev. A* **1992**, *45*, 2389.
(25) Onsager, L. *Ann. N.Y. Acad. Sci.* **1949**, *51*, 627.
(26) Sato, T.; Teramoto, A. *Macromolecules* **1996**, *29*, 4107.
(27) Abraham, F. F. *Phys. Rep.* **1979**, *53*, 93.
(28) Cui, S.-M.; Akcakir, O.; Chen, Z. Y. *Phys. Rev. E* **1995**, *51*, 4548.
(29) Grosberg, A. Y.; Pachomov, D. V. *Liq. Cryst.* **1991**, *10*, 539.
(30) Cotter, M. A. *Phys. Rev. A* **1974**, *10*, 625.
(31) Cotter, M. A. *J. Chem. Phys.* **1977**, *66*, 1098.

MA980697X